ISSN 1674-1056
http://cpb.iphy.ac.cn
http://iopscience.iop.org/cpb
中国物理 B
Chinese Physics
中国物理
Chinese Physics B

Surface plasmon polaritons frequency-blue shift in low confinement factor excitation region

Ling-Xi Hu(胡灵犀), Zhi-Qiang He(何志强), Min Hu(胡旻), and Sheng-Gang Liu(刘盛纲)
Citation: Chin. Phys. B, 2021, 30 (**8**): 084102. DOI: 10.1088/1674-1056/abe22e
Journal homepage: http://cpb.iphy.ac.cn; http://iopscience.iop.org/cpb

What follows is a list of articles you may be interested in

Cherenkov terahertz radiation from Dirac semimetals surface plasmon polaritons excited by an electron beam

Tao Zhao(赵陶), Zhenhua Wu(吴振华)
Chin. Phys. B, 2020, 29 (**3**): 034101. DOI: 10.1088/1674-1056/ab6840

Studies on convergence and scaling law of Thomson backscattering spectra in strong fields

Han-Zhang Xie(谢含章), Chun Jiang(蒋纯), Bai-Song Xie(谢柏松)
Chin. Phys. B, 2017, 26 (**12**): 124101. DOI: 10.1088/1674-1056/26/12/124101

Tunable coupling of a hybrid plasmonic waveguide consisting of two identical dielectric cylinders and a silver film

Benli Wang(王本立), Han Liang(梁涵), Jiafang Li(李家方)
Chin. Phys. B, 2017, 26 (**11**): 114103. DOI: 10.1088/1674-1056/26/11/114103

Spoof surface plasmon-based bandpass filter with extremely wide upper stopband

Xiaoyong Liu(刘小勇), Lei Zhu(祝雷), Yijun Feng(冯一军)
Chin. Phys. B, 2016, 25 (**3**): 034101. DOI: 10.1088/1674-1056/25/3/034101

Tunable terahertz radiation from arbitrary profile dielectric grating coated with graphene excited by an electron beam

Zhao Tao, Zhong Ren-Bin, Hu Min, Chen Xiao-Xing, Zhang Ping, Gong Sen, Liu Sheng-Gang
Chin. Phys. B, 2015, 24 (**9**): 094102. DOI: 10.1088/1674-1056/24/9/094102

Surface plasmon polaritons frequency-blue shift in low confinement factor excitation region*

Ling-Xi Hu(胡灵犀)[1,2], Zhi-Qiang He(何志强)[1,2], Min Hu(胡旻)[1,2,†], and Sheng-Gang Liu(刘盛纲)[1,2]

[1] *Terahertz Research Center, School of Electronic Science and Engineering, University of Electronic Science and Technology of China, Chengdu* 610054, *China*
[2] *Key Laboratory of Terahertz Technology, Ministry of Education, Chengdu* 610054, *China*

(Received 16 December 2020; revised manuscript received 12 January 2021; accepted manuscript online 2 February 2021)

Surface plasmon polaritons' (SPPs') frequency blue shift is observed in finite-difference time-domain (FDTD) simulation of parallel electron excitation Au bulk structure. Comparing with cold dispersion of SPPs, an obvious frequency blue shift is obtained in low confinement region excitation simulation results. Then, according to SPPs' transverse attenuation characteristics, the excited frequency mode instead of cold dispersion corresponding frequency mode matches it. Thence, this excited mode is confirmed to be SPPs' mode. As is well known the lower the frequency, the smaller the confinement factor is and the lower the excitation efficiency, the wider the bandwidth of excited SPPs is. And considering the attenuation in whole structure, the excited surface field contains attenuation signal. In a low confinement factor region, the higher the SPPs' frequency, the higher the excitation efficiency is, while broadband frequency information obtained in attenuation signal provides high frequency information in stimulation signal. Thence, in the beam–wave interaction, as the signal oscillation time increases, the frequency of the oscillation field gradually increases. Thus, compared with cold dispersion, the frequency of excited SPP is blueshifted This hypothesis is verified by monitoring the time domain signal of excited field in low and high confinement factor regions and comparing them. Then, this frequency-blue shift is confirmed to have commonality of SPPs, which is independent of SPPs' material and structure. Finally, this frequency-blue shift is confirmed in an attenuated total reflection (ATR) experiment. Owing to frequency dependence of most of SPPs' devices, such as coherent enhancement radiation and enhancement transmission devices, the frequency-blue shift presented here is of great influence in the SPPs applications.

Keywords: surface plasmon polaritons (SPPs), frequency-blue shift, surface plasmon resonance (SPR), coherent enhancement radiation

PACS: 41.60.–m, 41.60.Bq, 41.85.–p, 11.55.Fv **DOI:** 10.1088/1674-1056/abe22e

1. Introduction

Surface plasmon polaritons (SPPs) were observed in experiment as early as the 1900s[1] and the theoretical studies were subsequently conducted.[2–4] Owing to the improvement of nanotechnology and nanofabrication, SPPs have become a hot point of research again in recent years. The SPPs are the slow electromagnetic surface waves,[5,6] which are widely used in near-field imaging,[7–10] enhancement of optical transmission,[11–13] biosensors,[14–17] and enhancement of radiation.[18–20] The SPPs in metal or in advanced materials such as graphene, topological insulation excited in high confinement factor region (high frequency region) have been studied numerically.[21–24] However, there have been no specific researches of excited SPPs in low confinement factor region (low frequency region), which is SPPs' frequency rapid change region bringing excellent frequency tuning ability into the SPPs coherent enhanced radiation devices.[6,18,23,25]

Therefore, it is of great demands to study the excitation properties of SPPs in this excitation region. In this study, the finite-difference time-domain (FDTD) simulation is employed to investigate the excited electromagnetic field of SPPs' materials by parallel electrons. The parallel electron-excited Au bulk structure is calculated by solving Helmholtz's electromagnetic-field equation that is commonly used in theoretical analysis, in low confinement factor excitation region, and an obvious frequency-blue shift is observed in FDTD simulation results. According to SPPs' transverse attenuation characteristics,[5] this simulated excitation mode instead of cold dispersion frequency mode matches the attenuation property. Thence, this excited frequency-blue shift mode is confirmed to be SPPs' mode. As is well known the lower the frequency, the smaller the confinement factor is, and the lower the excitation efficiency, the wider the bandwidth of excited SPPs is.[5,18] And considering the attenuation in whole structure, the excitation signal contains more complex spectrum information attenuation signal. Owing to the property of high frequency signal easier to be excited and complex spectrum surface field attenuation signal, the hypothesis of excited SPPs' frequency-blue shift with excitation time increasing in low confinement factor region is proposed. Afterwards, this

*Project supported by the National Key Research and Development Program of China (Grant Nos. 2017YFA0701000, 2018YFF01013001, and 2020YFA0714001) and the National Natural Science Foundation of China (Grant Nos. 61988102, 61921002, and 62071108).

†Corresponding author. E-mail: hu_m@uestc.edu.cn

© 2021 Chinese Physical Society and IOP Publishing Ltd

hypothesis of frequency-blue shift is verified by analyzing the relationship between excitation frequency and the number of oscillation signal cycles in low and high confinement factor region, separately. Then, the excited SPPs' characteristics of film structure are studied, which is more widely used in practice.[7–20] And the results show that this frequency-blue shift of SPPs possesses the commonality in SPPs' low confinement factor region excitation, which is independent of material and structure. Finally, the frequency-blue shift is confirmed by attenuated total reflection (ATR) experiment. Owing to frequency dependence of most SPPs' devices, such as coherent enhancement radiation and enhancement transmission devices,[11–20] this excited frequency-blue shift presented here is of great influence in the SPPs applications.

2. SPPs' frequency-blue shift discovery and certification

The SPPs' frequency-blue shift in a low confinement factor region is firstly observed in the study of parallel electrons excited Au bulk. And the simulation model is shown in Fig. 1(a), which is a typical vacuum electrons excited Au bulk structure. The Drude model, which is a classical model proposed to explain the dielectric properties of metallic materials, is used to describe the relative permittivity of Au bulk, expressed as $\varepsilon_{\rm m} = \varepsilon_\infty - \omega_{\rm p}^2/(\omega^2 + {\rm j}\omega\gamma)$.[26,27] And the Drude parameters for Au are $\varepsilon_\infty = 8.9128$, $\omega_{\rm p} = 1.208 \times 10^{16}$ rad/s, $\gamma = 8.7894 \times 10^{13}$ Hz.[28,29] When electrons pass parallel across the metal surface, SPPs are excited on the surface. Thence, a series probes set at the interface between Au and vacuum are used to observe the information about the excited SPPs in simulation. And owing to the collective effect of material, the frequency corresponding to the strongest energy is considered as SPPs' frequency. Relationship between excitation frequency and excitation electron relative velocity $\beta = v/c$ forms dispersion relation, where v is the velocity of excitation electrons and c is light speed in vacuum. The simulation dispersion relation is shown in Fig. 1(b) and the detailed information about excitation frequency and relative velocity are presented in Table 1. And cold dispersion formula is calculated by solving Helmholtz's electromagnetic-field equation and boundary matching, and expressed as $k_{\rm SPPs} = k_0\sqrt{\varepsilon_{\rm m}/(1+\varepsilon_{\rm m})}$,[5] where $k_{\rm SPPs}$ is the wave vector of SPPs, $k_0 = \omega/c$ and ω is the angular frequency. The contrast cold dispersion relation is also shown in Fig. 1(b) and detailed information is presented in Table 1. In a high confinement factor region (high frequency region), excitation frequency is basically the same as cold dispersion result, while in low confinement factor region (low frequency region), an obvious blue shift of simulation excitation frequency is generated and the smaller the confinement factor, the more obvious the frequency-blue shift is.

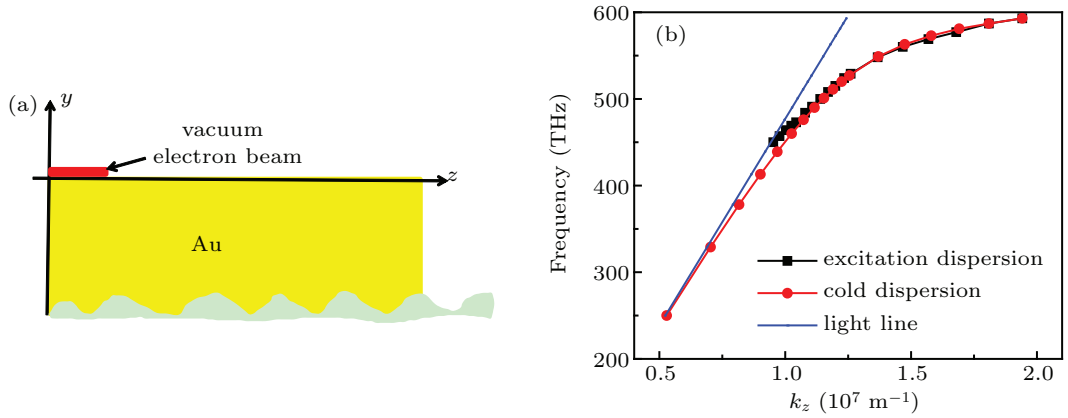


Fig. 1. (a) Scheme of parallel electrons excited Au bulk structure, and (b) cold dispersion (red) and simulation hot dispersion (black) curves of Au bulk, with light line (blue) in inset referring to vacuum light dispersion line, expressed as $k_z = \omega/c$.

Table 1. Relation of simulated and theoretically calculated cold dispersion frequency with excitation electron relative velocity.

β	0.64	0.68	0.72	0.76	0.8	0.84	0.88	0.89	0.9
Simulation (THz)	593	587	577	569	560	548	529	524	515
Cold dispersion (THz)	593	587	581	573	563	549	527	520	511
β	0.91	0.92	0.93	0.94	0.95	0.96	0.97	0.98	0.99
Simulation (THz)	508	500	491	484	473	469	464	457	450
Cold dispersion (THz)	501	490	476	460	439	413	378	329	250

Owing to its localization, the electromagnetic field of excited SPPs decays exponentially along the transverse direction. The attenuation length ratio of SPPs' mode in vacuum to that in metal is $R = L_{\rm Vacuum}/L_{\rm Au} = |\varepsilon_{\rm m}|$.[5] Then, the theoretical relationship between attenuation length ratio R and frequency is calculated and presented in Fig. 2(b). According

to the above excitation frequencies and theoretical frequencies in different excitation conditions, the simulation contour maps of these frequencies are obtained. The scheme of attenuation length ratio R in simulation contour map is shown in Fig. 2(a), and the frequency-dependent theoretical R and frequency-dependent R for cold dispersion and for excitation frequency are all presented in Fig. 2(b).

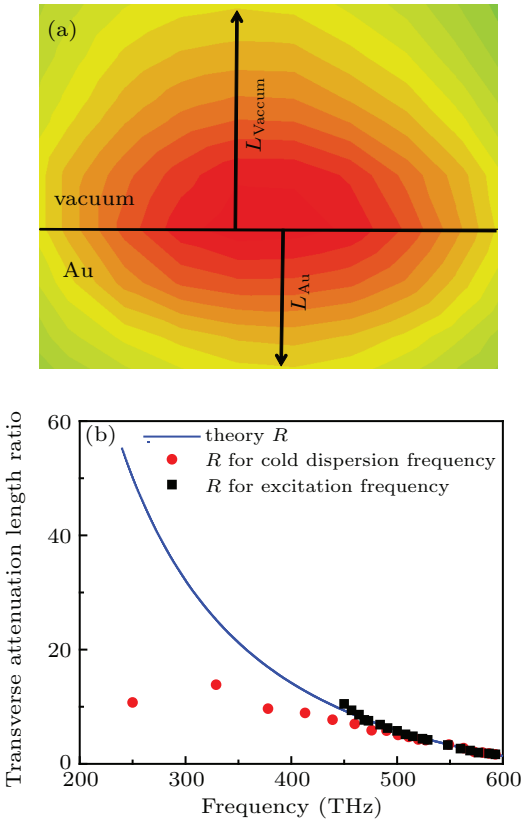


Fig. 2. (a) Scheme of attenuation length ratio R in simulation contour map (simulation contour map of 593 THz excited by 0.64c electrons); (b) Relationship curves between attenuation length ratio R and frequency (blue line: theoretical SPPs' attenuation ratio curve; red dots: simulation contour map attenuation ratio R for cold dispersion frequency; black square points: simulation contour map attenuation ratio R for excitation frequency).

Theoretical results show that SPPs' attenuation length ratio R increases with frequency decreasing. Therefore, as SPPs' frequency decreases, the confinement factor becomes less. The above results demonstrate that the transverse attenuation characteristic of excited frequency instead of cold dispersion frequency in simulation matches the theoretical SPPs' attenuation property. These results confirm that the excited mode is the SPPs' mode rather than cold dispersion frequency mode. And the excited SPPs' frequency blue shift in a low confinement factor region is also confirmed. The above results also show that the lower the SPPs' frequency, the greater the attenuation ratio value in vacuum and in metal is and the smaller the confinement factor at interface. Furthermore, the low confinement factor leads to low excitation efficiency and broadband field of excited SPPs. Owing to the broadband field property and high frequency SPPs easier to stimulate in a low confinement factor region, a hypothesis that the frequency of excited SPPs in low confinement factor region increases as the wave-beam interaction time increases can be proposed to comprehend this frequency-blue shift. Then, time domain signal of the probe at the interface is analyzed by the fast Fourier transform (FFT) to obtain the spectral characteristics of excited electromagnetic field and the relationship between frequency and number of stimulated signal cyclesin the 0.64c electrons' excitation condition (high confinement factor excitation condition) and 0.99c electrons' excitation condition (low confinement factor excitation condition) are presented in Tables 2 and 3, respectively.

In the high confinement factor region, as the number of signal cycles increases, the frequency of excited SPPs' signal in each cycle randomly changes near the strongest energy frequency, which is the excited SPPs' frequency. It is because of the numerical error of iterative process in simulation. But in the low confinement factor region, as the number of signal cycles increases, the frequency of excited SPPs keeps increasing. In the low confinement factor region, the higher the SPPs' frequency, the higher the excitation efficiency is, while the obtained broadband frequency information in structure attenuation signal provides high frequency information in the excited field. Thence, in the beam–wave interaction, as the signal oscillation time increases, the frequency of the oscillation field gradually increases. Owing to the collective effect of free electron oscillation, the frequency with the strongest energy is the excited SPPs' frequency. Compared with cold dispersion frequency, the frequency of excited SPPs is blue-shifted. The above hypothesis about the excited SPPs frequency blue shift is confirmed.

Table 2. Relationship between SPPs' signal frequency and number of signal cycles in 0.64c electron excitation condition.

Cycle's number	1	2	3	4	5	6	7	8	9
Frequency (THz)	596	595	591	587	598	588	589	595	594

Table 3. Relationship between excited SPPs' signal frequency and number of signal cycles in 0.99c electrons excitation condition.

Cycle's number	1	2	3	4	5	6	7	8	9
Frequency (THz)	372	407	430	445	460	472	483	493	502

3. Excited SPPs' frequency characteristics in metal film structure

The excited SPPs' frequency-blue shift in the low confinement factor region of metal bulk structure excited by parallel electrons is confirmed and comprehended. The lower frequency with lower stimulation efficiency and broader bandwidth leads the frequency to increase with the oscillation of the excitation signal field, which causes the excited SPPs' frequency to be blue-shifted in the low confinement factor region. Considering the fact that most of SPPs' applications used are the thin film structures, such as SPPs' coherent enhancement radiation or attenuated total reflection (ATR) biochemical sensors,[11–20,30] and the above reason for frequency blue shift still exists in film structure, the SPPs' excitation characteristics in metal film structure are studied in this paper. A parallel electron beam stimulated metal film with a dielectric substrate, which is a typical structure to coherently enhance Cherenkov radiation by the excited SPPs in metal film[18] is employed in this study and the structure scheme is shown in Fig. 3(a). The cold dispersion of 50-nm-thick Au film spin-coated on the dielectric substrate is calculated and the dispersion curves are shown in Fig. 3(b). The relative permittivity of substrate is set to be 9 and Drude parameters of Au film are set to be as follows: $\varepsilon_\infty = 8.9128$, $\omega_p = 1.208 \times 10^{16}$ rad/s, and $\gamma = 8.7894 \times 10^{13}$ Hz.[28,29] It is clear that there are two SPPs' modes in film structure: the SPPs' symmetric (even) mode and SPPs asymmetric (odd) mode. When the energy of excitation electrons is higher than the Cherenkov radiation threshold (electron velocity higher than the light speed in substrate dielectric) of the substrate, only asymmetric mode can be stimulated in this structure. And owing to the low excitation efficiency of SPPs in the low confinement factor region, only asymmetric mode is discussed in this study. Then, 50-nm-thick Au and Ag film structures are investigated in simulation and the results are presented in Figs. 3(c) and 3(d), respectively. The Drude parameters of Ag film are given as follows: $\varepsilon_\infty = 5.9833$, $\omega_p = 1.4772 \times 10^{16}$ rad/s, and $\gamma = 1.4276 \times 10^{14}$ Hz.[28,29] The excited SPPs' frequency-blue shift in the low confinement factor region is observed in both of the above structures. All the above results verify that this frequency-blue shift possesses the commonality of SPPs, which is independent of structure and material. The frequency-blue shift leads the dispersion to be modified and unavailable from the low frequency SPPs, which means that a low cutoff frequency is generated. And the low cutoff frequency of excited SPPs depends on the limit SPPs' frequency at the maximum wave vector. For the 50-nm-thick Au film structure, the limit SPPs' frequency is about 610 THz while the low cutoff frequency is about 450 THz, and for Ag, the limit SPPs' frequency is 880 THz while the low cutoff frequency is about 500 THz.

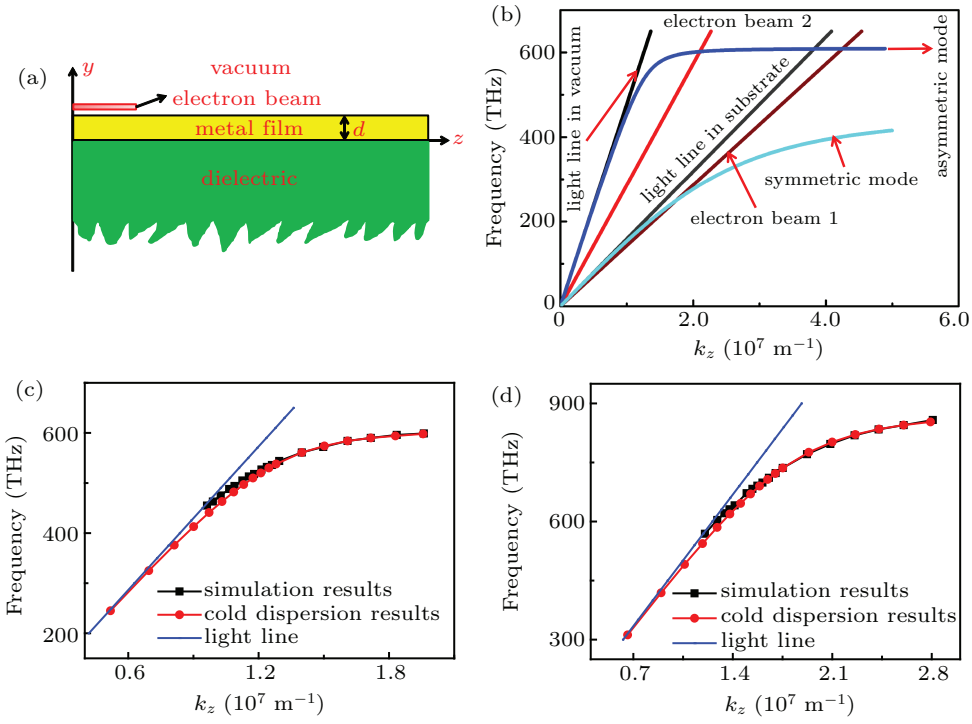


Fig. 3. (a) Scheme of parallel electrons stimulated metal film structure. (b) Cold dispersion curves of 50-nm-thick Au film spin-coated on dielectric substrate with relative permittivity 9. In panels (a) and (b) black curve is symmetric mode, red curve refers to asymmetric mode, blue straight line represents light dispersion line in vacuum (expressed as $k_z = \omega/c$), and magenta straight line denotes light dispersion line in dielectric substrate (expressed as $k_z = n\omega/c$), with n is refractive index of dielectric substrate. (c) Simulation and cold dispersion curves of 50-nm-thick Au film coated on the dielectric substrate with relative permittivity 9, with light line in the legend referring to to vacuum light dispersion line and expressed as $k_z = \omega/c$. (d) Simulation and cold dispersion curves of 50-nm-thick Ag film coated on the dielectric substrate with relative permittivity 9, with light line in the legend referring to vacuum light dispersion line and expressed as $k_z = \omega/c$.

Finally, this SPPs' frequency-blue shift is confirmed in a microwave excitation attenuated total reflection (ATR) experiment[30] in which used is a typical Kretschmann structure, and the experimental setup is presented in Fig. 4(a). A 40-nm-thick Au film is spin-coated on a semi-cylindrical fused silica substrate (ATR structure) and xenon light source is employed in this experiment. The schematic diagram of light path is shown in Fig. 4(b). The broadband light of xenon lamp is connected to a collimator through an optical fiber, and thus forming a parallel light beam. This parallel light beam passes through a polarizer and diaphragm and reaches an ATR structure, then, the reflection light is collected by a collimator and transmitted via optical fiber to a spectrometer. As is well known the SPPs' microwave mode is the TM mode. By adjusting the polarization of the incident light, the observed weakest spectrum is of TM mode and the strongest spectrum is of TE mode. Then, the absorption peak frequency obtained by dividing these two spectra is the excited SPPs' frequency in experiment. The excited SPPs' longitudinal wave vector in this ATR structure satisfies this formula: $k_{\mathrm{SPPs}} = nk_0 \sin\theta$, where n is the refractive index of silica substrate and θ is the incident angle. The scheme of the ATR structure is shown in Fig. 4(c). The dispersion relationship can be obtained by adjusting the incident angle. The excited SPPs' dispersion relationship in experiment and simulation and cold dispersion and also their comparisons are shown in Fig. 4(d). The experimental results are basically consistent with the simulation results. Thence, the excited SPPs' blue shift in low confinement factor region is confirmed in this experiment.

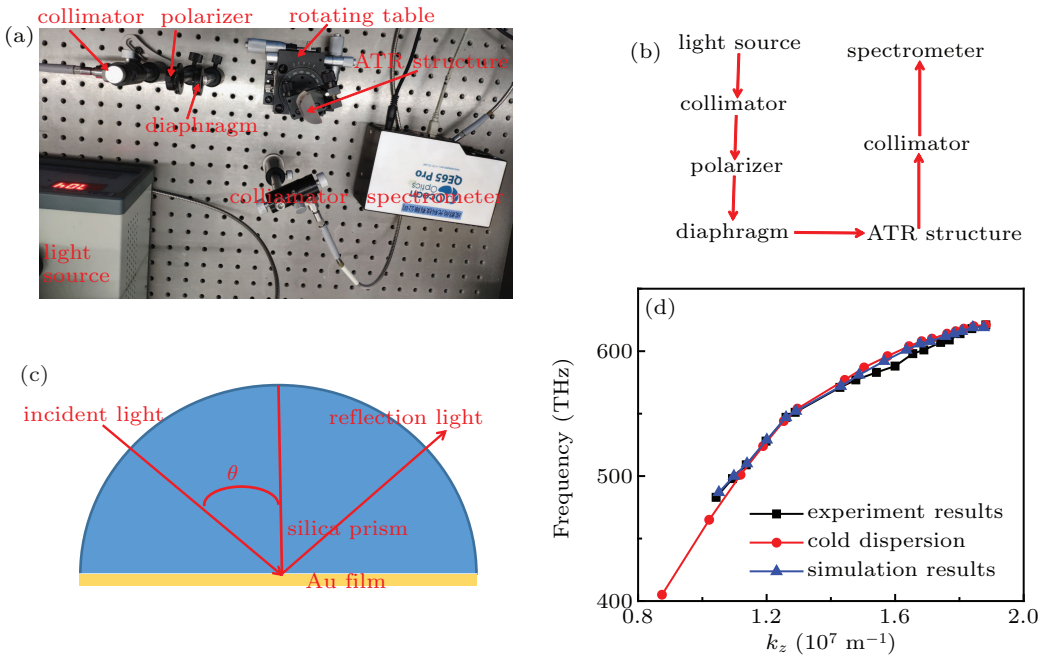


Fig. 4. (a) ATR experimental setup, (b) light path scheme, (c) scheme of ATR structure, and (d) dispersion curves of experimental, simulation results, and cold dispersion and their comparisons.

4. Conclusions and perspectives

Dispersion characteristics are the essential electromagnetic properties of materials. In this research, excited SPPs' frequency-blue shift is observed in a low confinement factor region by analyzing the finite-difference time-domain (FDTD) simulation results and cold dispersion results of electromagnetic wave boundary match about Au bulk structure. And according to SPPs' transverse field attenuation characteristics in Au bulk, the excited frequency-blue shift mode is confirmed to be the SPPs' mode. Owing to the property of high frequency signal easier to excite and complex spectrum surface field attenuation signal, the hypothesis that the excited SPPs' frequency-blue shift increases with excitation time increasing in low confinement factor region is proposed. And then, this hypothesis of frequency-blue shift is verified by analyzing the relationship between excitation frequency and the number of oscillation signal cycles in low and high confinement factor regions, respectively. Afterwards, this frequency-blue shift is confirmed to possess the commonality of SPPs, which is independent of SPPs' material and structure in the study of 50-nm-thick Au and Ag films with substrate. Finally, the attenuated total reflection (ATR) experiment confirms this frequency-blue shift. Owing to the frequency dependence in most of SPPs' devices, such as coherent enhancement radiation and enhancement transmission devices, this excited frequency-blue shift presented here is of great significance in the SPPs' applications.

References

[1] Wood R W 1902 *Phil. Mag.* **18** 4

[2] Fan U 1941 *Opt. Soc. Am.* **31** 3
[3] Ritchie R H 1957 *Phys. Rev.* **106** 5
[4] Stern E A and Ferrell R A 1960 *Phys. Rev.* **120** 1
[5] Reather H 1988 *Surface Plasmons on Smooth Surfaces* (Berlin: Springer Tracts in Modern Physics) pp. 4–39
[6] Abajo F J G 2010 *Rev. Mod. Phys.* **82** 3
[7] Pendry J B 2000 *Phys. Rev. Lett.* **85** 18
[8] Pohl D W 2001 *Near-Field Optics and the Surface Plasmon Polariton* (Berlin: Topics in Applied Physics) pp. 1–13
[9] Zayats A V and Smolyaninov I I 2003 *J. Opt. A, Pure Appl. Opt.* **5** S16
[10] Fang N, Lee H, Sun C and Zhang X 2005 *Science* **308** 5721
[11] Ghaemi H F, Thio Tineke, Grupp D E, Ebbesen T W and Lezec H J 1998 *Phys. Rev. B* **58** 11
[12] Barnes W L, Dereux A and Ebbesen T W 2003 *Nature* **424** 6950
[13] Gan F Y, Wang Y J, Sun C W, Zhang G R, Li H Y, Chen J J and Gong Q H 2017 *Adv. Opt. Mater.* **5** 1600545
[14] Homola J, Yee S S and Gauglitz G 1999 *Sensor Actuat. B: Chem.* **54** 1
[15] Zhong Y T, Cheng Z Q, Ma L, Wang J H, Hao Z H and Wang Q Q 2014 *Chin. Phys. Lett.* **31** 047302
[16] Steinke N, Döring S, Wuchrer R, Kroh C, Gerlach G and Härtling T 2019 *Sensor Actuat. B: Chem.* **288** 594
[17] Han F, Lang T T, Mao B N, Zhao C L, Kang J, Shen C Y and Wang D N 2019 *Opt. Fiber Technol.* **50** 172
[18] LiuS G, Zhang P, Liu W H, Gong S, Zhong R B, Zhang Y X and Hu M 2012 *Phys. Rev. Lett.* **109** 153902
[19] Gong S, Hu M, Zhong R B, Chen X X, Zhang P, Zhao T and Liu S G 2014 *Opt. Express* **22** 16
[20] Liu S G, Zhang C, Hu M, Chen X X, Zhang P, Gong S, Zhao T and Zhong R B 2014 *Appl. Phys. Lett.* **104** 201104
[21] Gong S, Zhong R B, Hu M, Chen X X, Zhang P, Zhao T and Liu S G 2015 *Chin. Phys. B* **24** 077302
[22] Gong S, Hu M, Zhong R B, Zhao T, Zhang C and Liu S G 2017 *Opt. Express* **25** 21
[23] Hu L X, Gong S, Hu M, Zhong R B, Zhao T and Liu S G 2019 *Opt. Commun.* **433** 195
[24] Suo P F, Mao L and Xu H X 2020 *Chin. Phys. Lett.* **37** 017801
[25] Apsimon R J, Flower P S, Freeston K A, Hallewell G D, Morris J A G, Morris J V, Palerson C N, Sharp P H, Uden C N, Davenport M, Eades J, Coyle P A, Mercer D, Danaher S, McClatchey P H, Thacker N and Thompson L F 1986 *IEEE Trans. Nucl. Sci.* **33** 1
[26] Drude P 1960 *Ann. Phys.* **306** 3
[27] Ashcroft N W and Mermin N D 1976 *Solid State Physics* (New York: Saunders College Publishing) pp. 107–134
[28] Sondheimer E H 1952 *Adv. Phys.* **1** 1
[29] Johnson P B and Christy R W 1972 *Phys. Rev. B* **6** 12
[30] Kretschmann E J and Reather H 1968 *Verlag der Zeitschrift für Naturforschung A* **23** 12